

Supplement of Nat. Hazards Earth Syst. Sci., 19, 455–469, 2019  
<https://doi.org/10.5194/nhess-19-455-2019-supplement>  
© Author(s) 2019. This work is distributed under  
the Creative Commons Attribution 4.0 License.



*Supplement of*

## **From regional to local SPTHA: efficient computation of probabilistic tsunami inundation maps addressing near-field sources**

**Manuela Volpe et al.**

*Correspondence to:* Manuela Volpe ([manuela.volpe@ingv.it](mailto:manuela.volpe@ingv.it))

The copyright of individual parts of the supplement might differ from the CC BY 4.0 License.

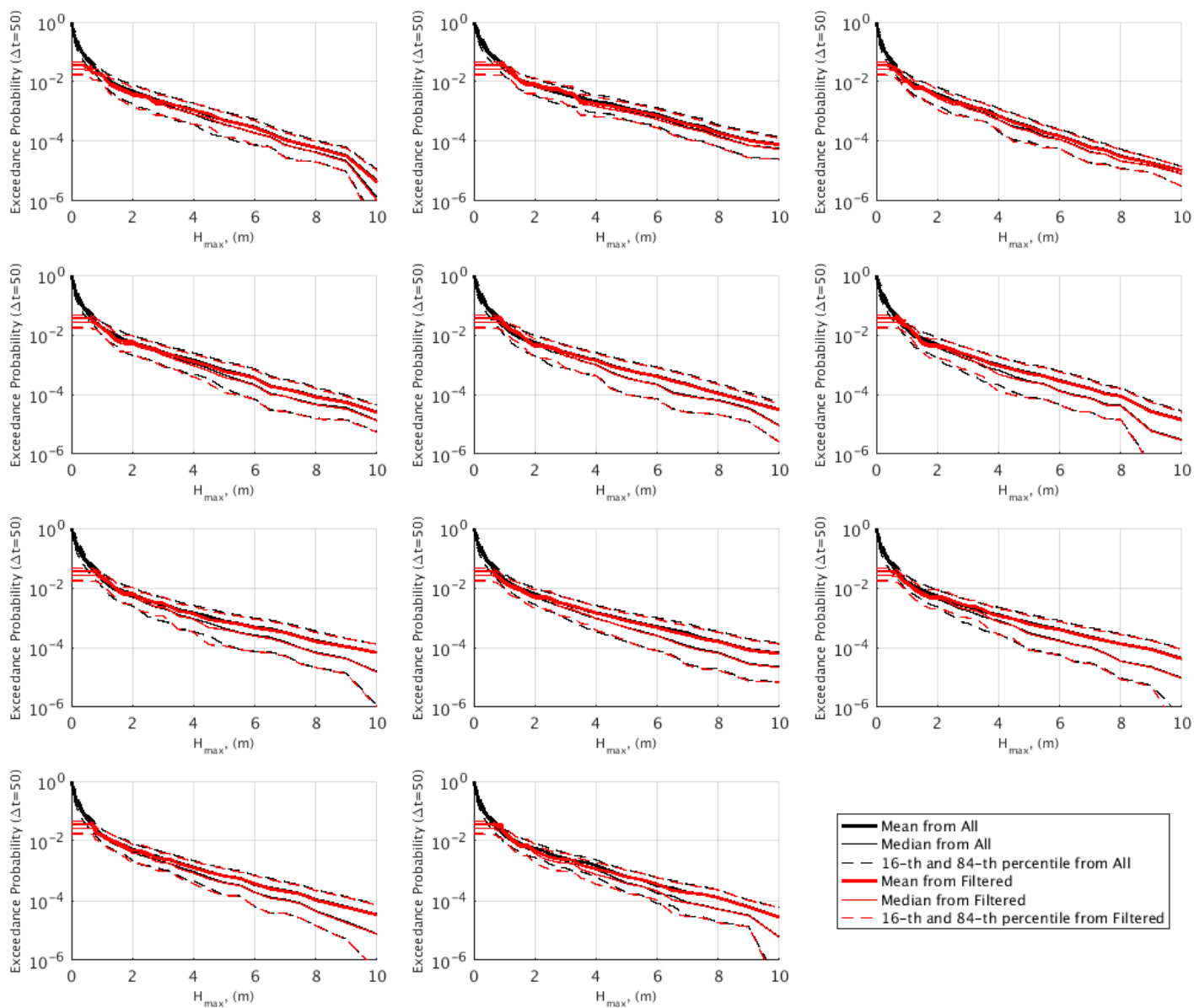


**Figure S1.** Offshore hazard curves at the 11 control points as obtained from the original and the filtered set of sources. The mean as well as some significant quantiles of the epistemic uncertainty are shown.

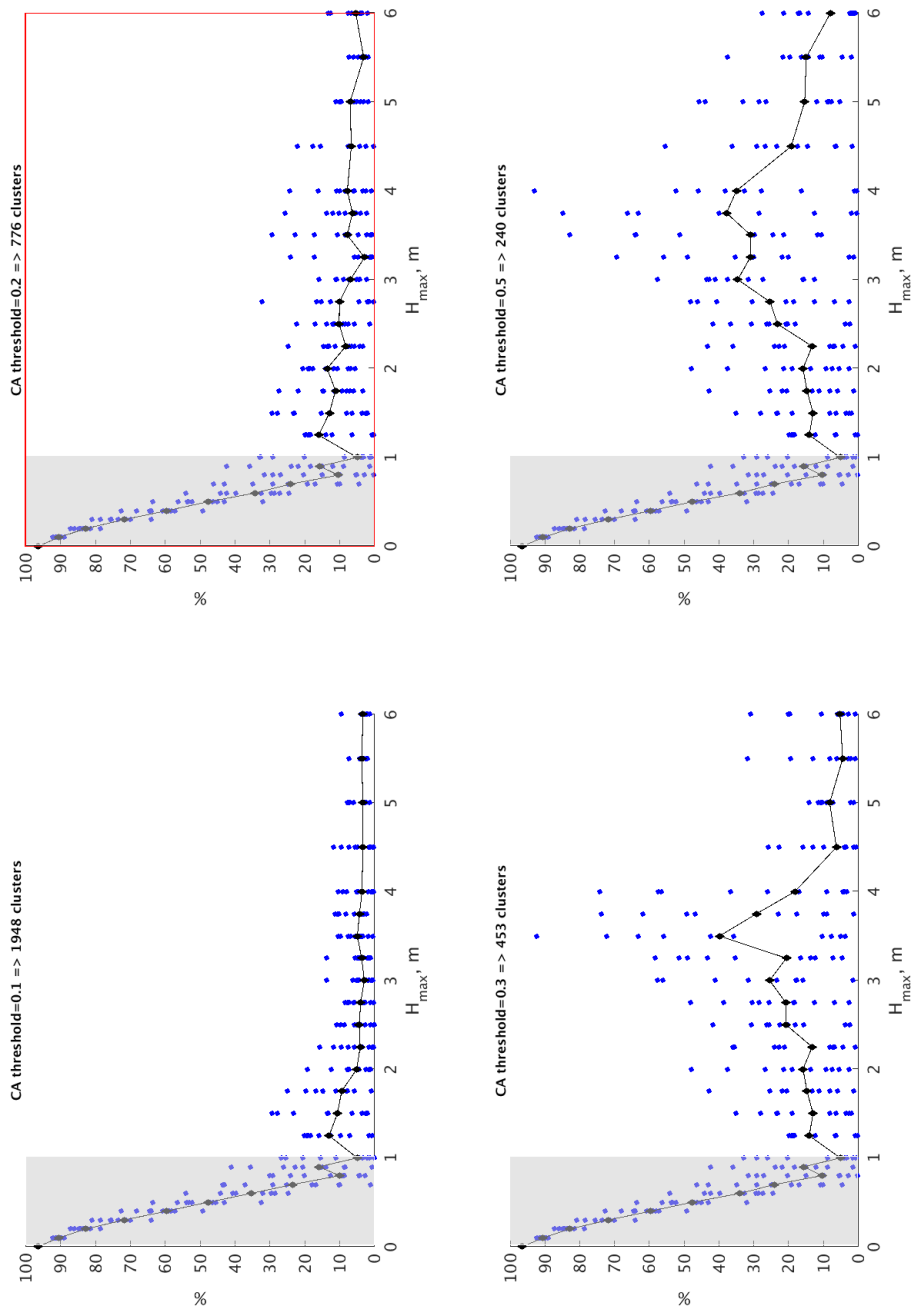


**Figure S2.** Sensitivity analysis (for step (3a)) concerning the cluster analysis threshold, showing the percentage differences between the offshore hazard curves computed from the original and the filtered set of sources, for different tsunami intensities. The higher is the threshold, i.e. the stronger is the imposed constraint, the more accurate is the clustering, to the detriment of the number of clusters. On the contrary, lower thresholds lead to less clusters but enlarge the errors. The red box corresponds to the value adopted in this study.

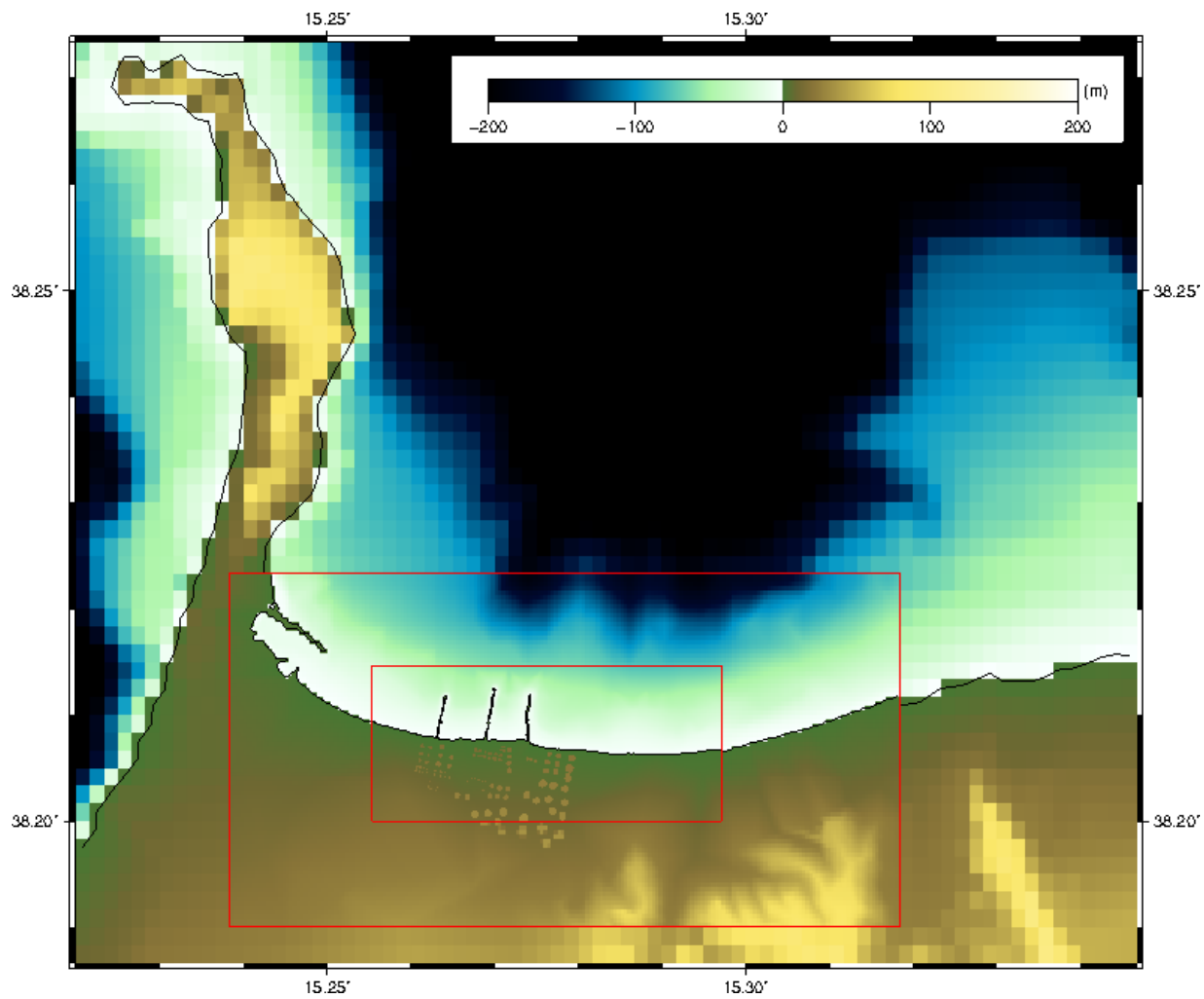


**Figure S3.** Close-up view of the topo-bathymetric nested grids used for tsunami simulations, with gradually increasing resolution (0.1, 0.025, 0.00625 arc-min). The domain of the outer grid (0.4 arc-min) is the one showed in Fig. 2 of the manuscript.

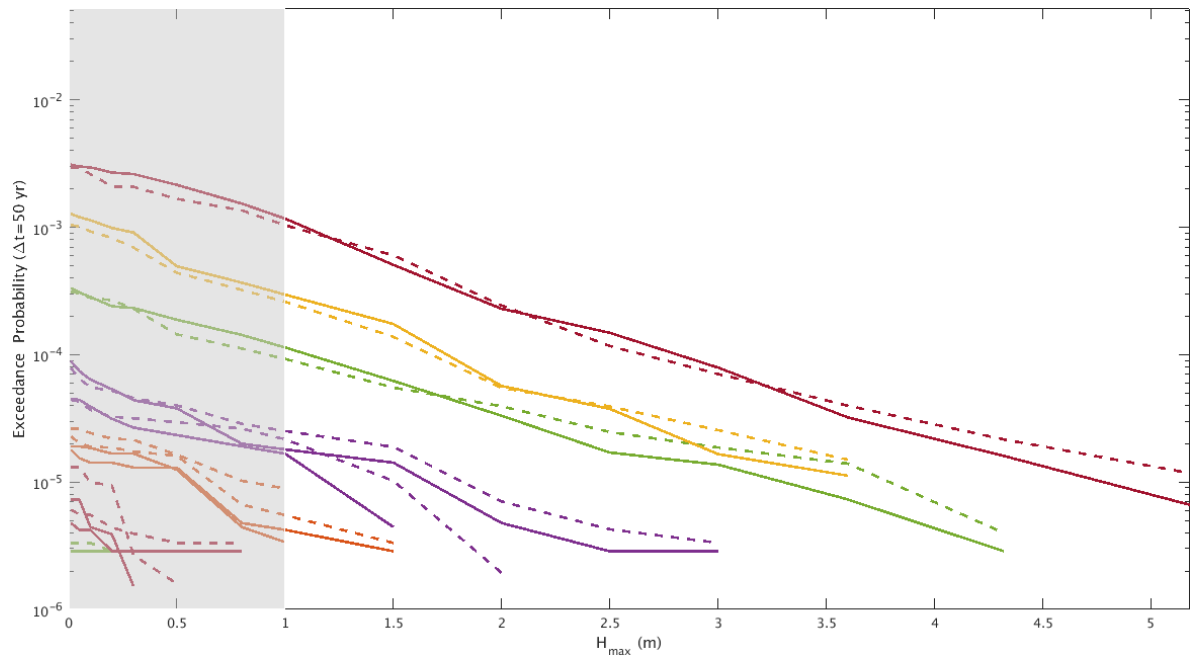


**Figure S4.** Mean hazard curves for  $H_{max}$  at few inland points within the highest resolution grid, as obtained from step (3a) (dashed lines) and step (3b) (plain lines) of the SPTHA procedure.

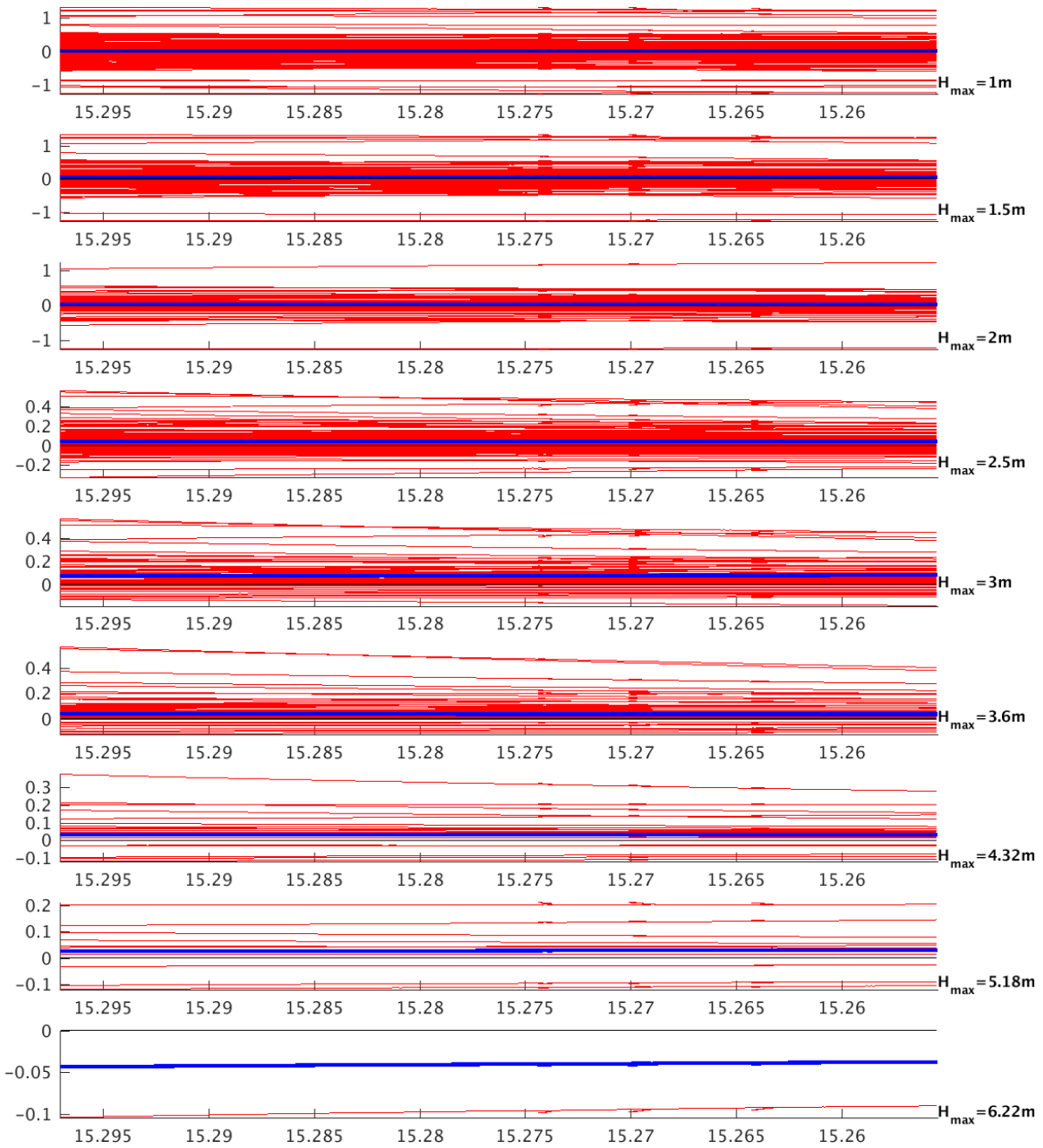


**Figure S5.** Red lines: coseismic displacements along the coastline of the higher resolution grid produced by each representative scenario contributing to different  $H_{max}$  values ( $\geq 1m$ ). Blue lines: weighted averages on all the scenarios.

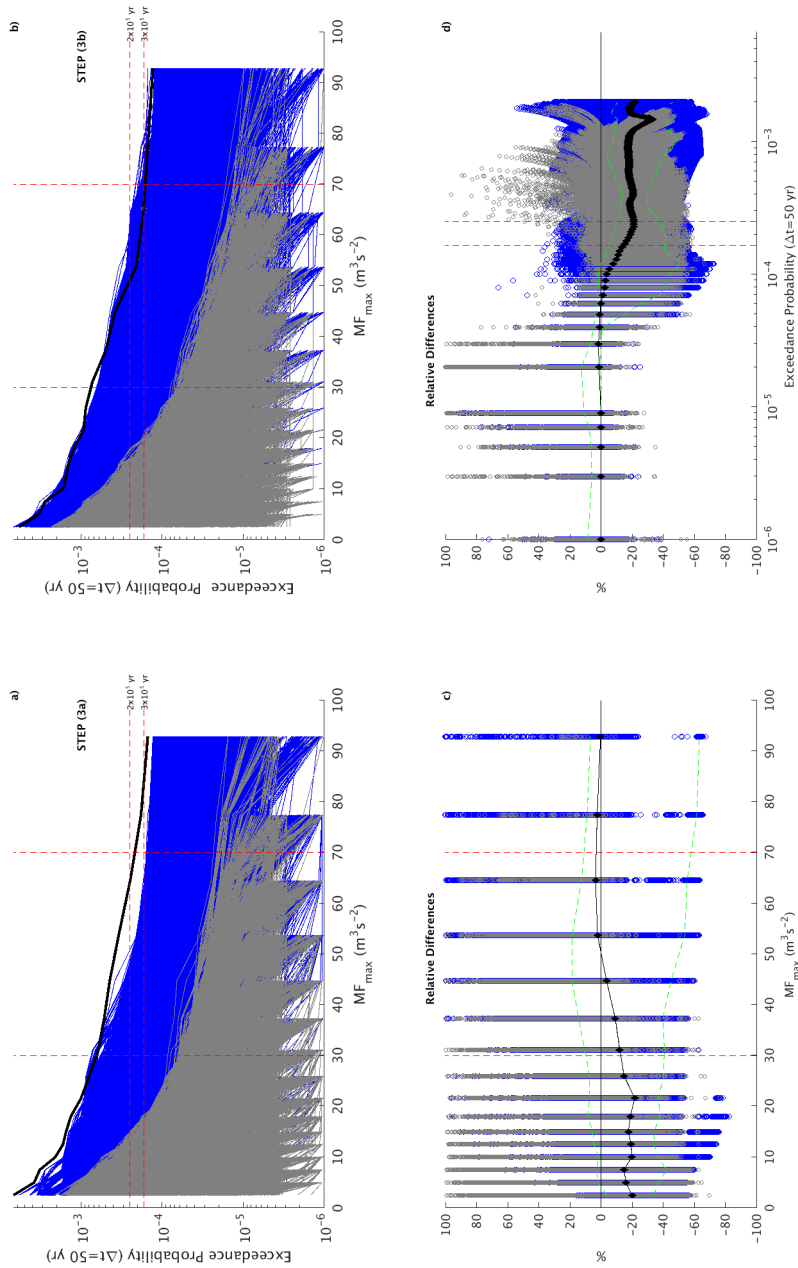


**Figure S6.** a) Mean hazard curves for  $MF_{max}$  at all points within the highest resolution grid, as obtained from step (3a) of the SPTHA procedure (see text and Fig. 1). Grey and blue colors refer to inland and offshore points, respectively. The bold black line represents the envelope of the curves from step (3b). Red dashed lines represent the values used to obtain probability (Fig. S7) and hazard (Fig. S8) inundation maps. b) Same as a) but using step (3b). The bold black line is the envelope of the curves from step (3a). c) Relative differences in terms of exceedance probability (in 50yr) as a function of  $MF_{max}$ , computed as  $[(3a) - (3b)] / (3b)$ . The black line is the median of the point distribution; the green dashed lines correspond to the 16<sup>th</sup> and 84<sup>th</sup> percentile. d) Same as c) but in terms of  $MF_{max}$  as a function of the exceedance probability (in 50yr).

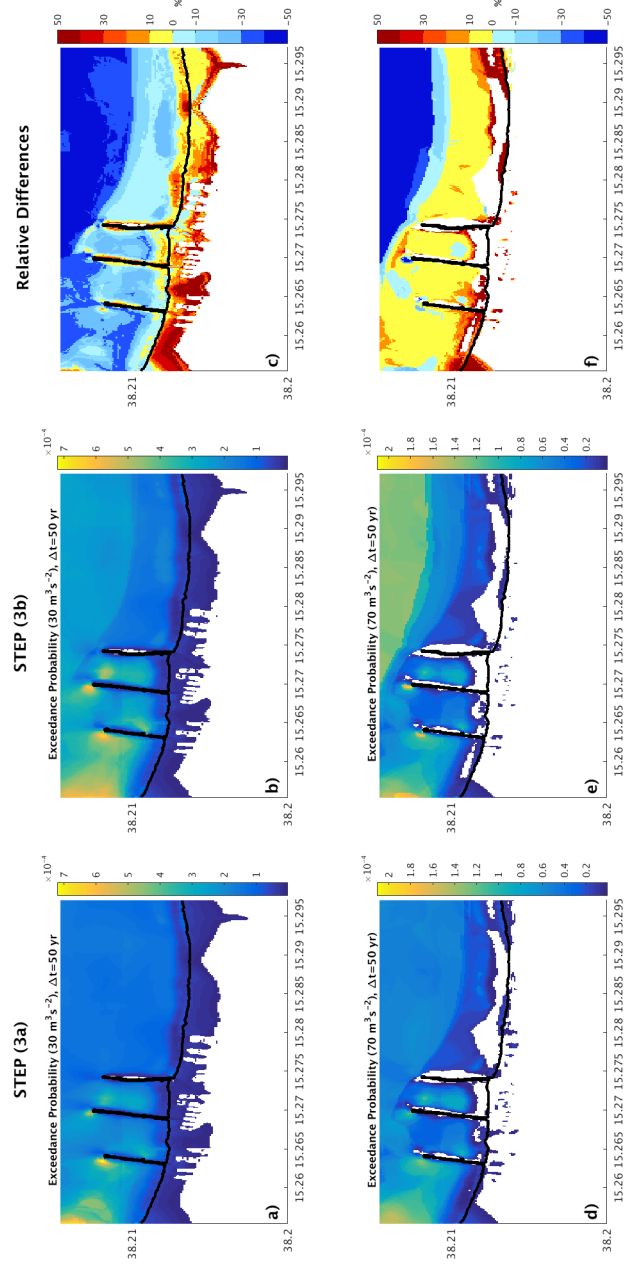


**Figure S7.** Probability maps (inner grid) for  $MF_{max}$  derived from the hazard curves in Fig. S6 at two different thresholds ( $30m^3s^{-2}$ ,  $70m^3s^{-2}$ ) for step (3a) and (3b) and relative differences computed as  $[(3a) - (3b)]/(3b)$ .



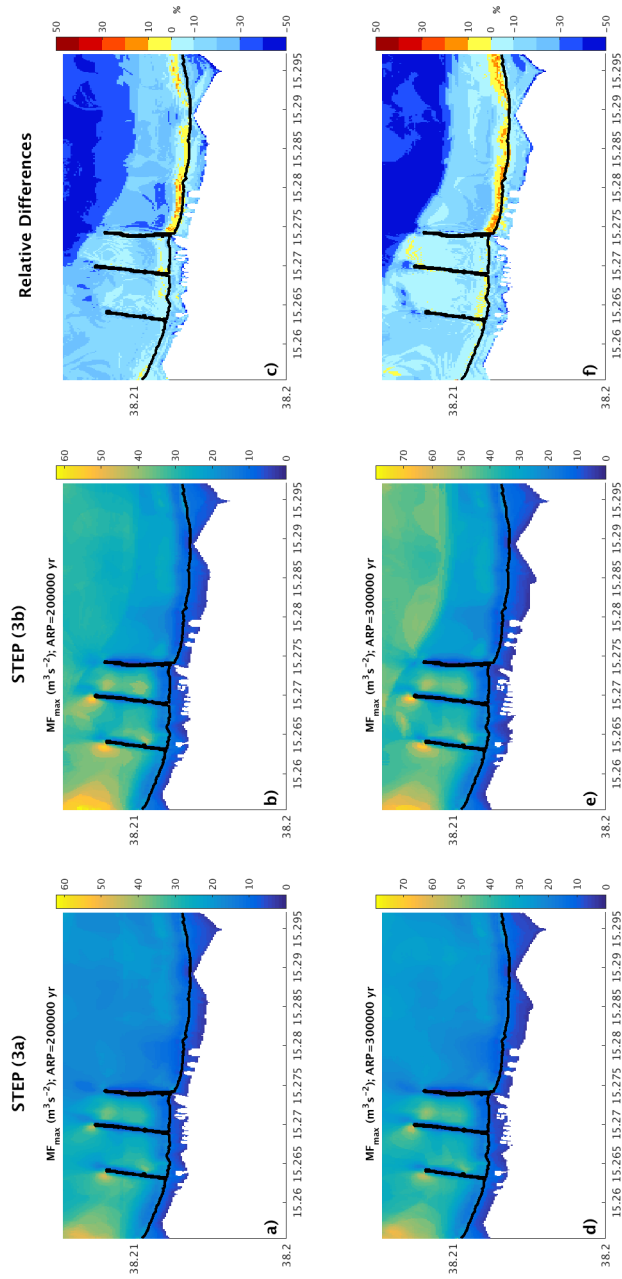


**Figure S8.** Hazard maps (inner grid) for  $MF_{max}$  derived from the hazard curves in Fig. S6 at two different ARPs ( $2 \times 10^5 yr$ ,  $3 \times 10^5 yr$ ) for step (3a) and (3b) and relative differences computed as  $[(3a) - (3b)] / (3b)$ .